JOM, Vol. 67, No. 2, 2015
DOI: 10.1007/s11837-014-1270-y

Characterization and Origin of Zonal Sapphire from Shandong Province, China

XIAOYAN YU,[1,4] XIAOWEI NIU,[2] and LINGHAO ZHAO[3]

1.—School of Gemology, China University of Geosciences, Beijing, China. 2.—Institute of Analytical and Testing Technology, General Research Institute for Nonferrous Metals, Beijing, China. 3.—National Research Center for Geoanalysis, Chinese Academy of Geology Science, Beijing, China. 4.—e-mail: yuxy@cugb.edu.cn

Shandong Province is the main producer of sapphire in China. Among the sapphire deposits discovered in China, Shandong sapphire hosted in Cenzoic basalt shows a great variety of features, especially for in zoning. These sapphire crystals are generally large in size, with depth in color and well-developed zoning. In this article, the characteristics of zonal sapphire have been studied by using petrography, trace element data from laser ablation inductively coupled with plasma-mass spectrometry, and Raman spectrometry. The trace elements variation is proposed to correspond with their parent magma composition, and the changes in growth environment of sapphire have resulted in the formation of zoning features. Sapphires from different geological settings have different characteristics. Trace elements in sapphire not only affect the color but also reflect the changes of physical and chemical conditions of sapphire growth. The concentration of impurity elements in the zoning core of Shandong sapphire is the highest, indicating that the parent magma of Shandong sapphire-host basaltic rock is rich in trace elements. Fe content is more than 2.00% in the zoning core, which causes the deepest color in the samples. It also suggests that the total content of Fe is positively correlated to the band color. The Raman spectrum shows that the spectrum peaks at 246 cm^{-1} caused by Fe^{3+} vary regularly with the band color, which shows that Fe is dominated by Fe^{3+} in Shandong sapphire. With the changes of forming condition, the parent magma composition has changed accordingly, which causes the zoning formation.

INTRODUCTION

Several sapphire deposits have been found in China, mainly distributed in Heilongjiang,[1] Shandong, Jiangsu, Fujian, and Hainan provinces.[2] The sapphire deposit in Shandong is large in scale and produces a great variety of sapphires. The deposit is located to the west of Tan-Lu fault zone, southeast of the North China Craton. It is in the geologically active region in eastern China featured with remarkable mantle upwelling and crust thinning in the Mesozoic and Cenozoic era.[3] The primary sapphire is hosted in Cenozoic basalts in Fangshan and Wutu towns. The secondary deposit occurred in the old channel deposit under the Quaternary sediments adjacent to Fangshan. Corundum megacryst crystallizes in the early alkaline basaltic magma in a deep source of high pressure. The host basalt contains alkali, high Al and low Si.[4,5]

For sapphire, a tremendous amount of research has investigated the chemical composition, crystal structure, physical properties,[6] and color mechanism,[7,8] and it has advocated for several different genetic types,[9–11] but there is still controversy on its origin. In recent years, with the advancement of analytical instruments, researchers have made further studies on sapphire, such as testing inclusion density by Raman[12] and detecting trace elements by laser ablation inductively coupled with plasma-mass spectrometry (LA-ICP-MS).[14] LA-ICP-MS has been widely used in the analysis of mineral trace elements. Contents and/or ratios of some trace elements that could indicate correlative geological

(Published online January 6, 2015)

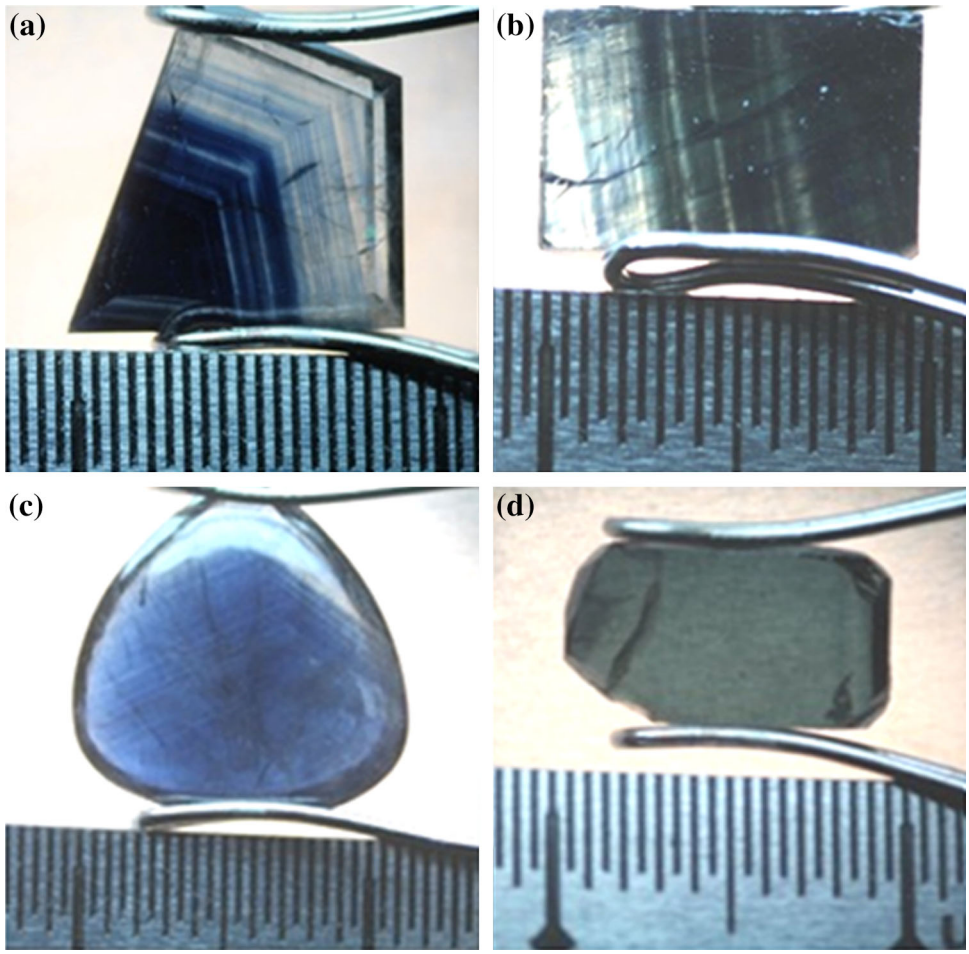

Fig. 1. Sample photos, the calibration of scale is 0.5 mm: (a) sample SC1 (b) sample SC2, (c) sample SC3, and (d) sample SC4. The sample photos were taken in the dark-field lighting condition of gem microscope.

processes are also important indicators in mineral origin. Zoning is one of the prominent characteristics of Shandong sapphire; its existence is associated with the environmental changes in crystal growth. By using LA-ICP-MS and Raman testing methods, the detailed variation of trace elements in zonal sapphire is characterized in this article.

MATERIALS AND METHODS

Samples and Conventional Observation

Four sapphire samples of deep blue and greenish-blue from Shandong were selected, namely SC1, SC2, SC3, and SC4. Sample SC1 was deep blue and light blue with well-developed angular zoning and a dark blue core. Sample SC2 was deep greenish-blue and light greenish-blue, and it displayed parallel zoning. Most zoning width was narrow at approximately 0.01–0.15 mm, and superimposition of zones can be seen (Fig. 1b). Samples SC3 and SC4 were contrast samples of the same color without zoning to SC1 and SC2.

Conventional gemological testing of sapphire samples was completed at Gem Testing Laboratory in the Gemological Institute, China University of Geosciences (Beijing, China). Dichroism of samples was tested with a handheld dichroscope under white light. The colors were observed in directions parallel and perpendicular to the *C* axis of the sapphire crystals. The samples have polished bent or plane surfaces. The refractive index of sample SC3 was tested by the distant vision method with the refractometer, whereas other three samples were tested by the facet method. The relative density of the samples was tested by the hydrostatic method; each sample was tested three times and the results were averaged. The absorption spectra were measured by the transmission method with a handheld prism spectroscope.

LA-ICP-MS ANALYSIS

LA-ICP-MS analysis is a qualitative and quantitative analysis of detecting the excited elements on the upper surface of a tiny area on the sample.[15] In this article, the LA-ICP-MS experiment was used to determine the types and contents of trace elements from different zones to analyze the distribution of elements and to provide a basis to discuss the origin of zonal sapphire crystals.

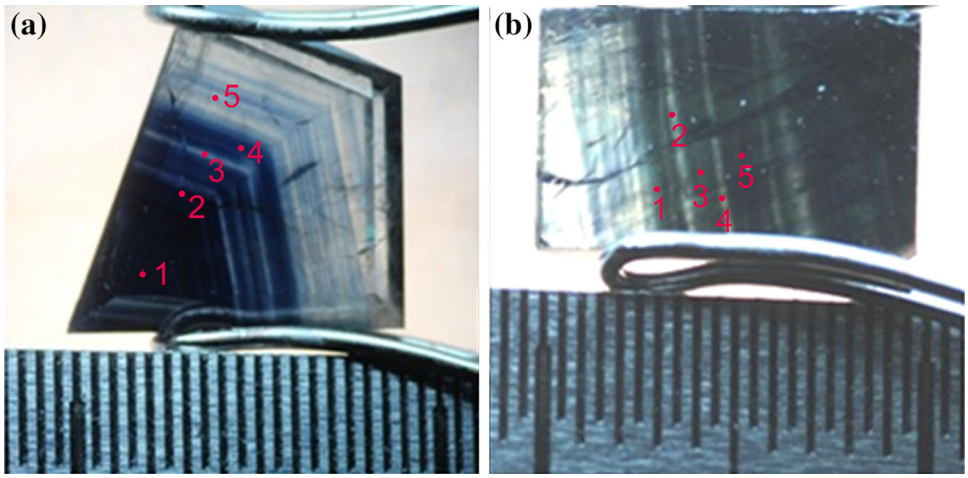

Fig. 2. Dotting position of samples by LA-ICP-MS: (a) dotting sequence of sample SC1 and (b) dotting sequence of sample SC2.

The experiment was conducted at the National Research Center for Geoanalysis, Chinese Academy of Geology Science. LA-ICP-MS (element 2) was used with ArF excimer laser. The laser wavelength was 193 nm, the laser spot beam was 35 μm, the frequency was 10 Hz, and the laser energy was 80%. The data were processed by Al standard, using the multiple external standard matrix to a certain amount, with the standard sample of NIST612/NIST610. The basic principle of the internal element compensation standard is the relative sensitivity between calibration instrument and unknown samples remain unchanged.[16]

As shown in Fig. 2, sample SC1 developed angular blue zoning; the dotting sequence extended from the zoning core to the edge. Sample SC2 developed parallel greenish-blue zoning, with alternative bands of deep and light colors. This sample developed close and narrow bands with overlaps; thus, the dotting position might have been caused by deviation. Five component points were selected from each sample of SC1 and SC2. Sample SC3 was uniform deep blue. SC4 was consistent deep greenish-blue color. They were contrast samples to SC1 and SC2; one component point was selected from each sample.

Raman Spectrum Test

Laser confocal Raman spectrometer (Lab RAM HR Evolution) was used in the Research Center of Material Science, Tsinghua University, Beijing, China, at room temperature with the excitation light source of λ = 532 nm, sample power of 50 mW, and scanning wave number range of 200–1200 cm^{-1}.

Samples SC1 and SC2 were selected for analysis. Sample SC1 developed angular blue zoning, and the dotting sequence extended from the zoning core to the edge of six component points. Sample SC2 developed parallel greenish-blue zoning. Two component points from this sample were selected from deep- and light-colored bands.

RESULTS

Conventional Testing

For all samples, the refractive index values ranged from 1.760 to 1.772, and the double refractive index varied from 0.008 to 0.010. The dichroism was blue to greenish-blue/green. A 450-nm absorption band and 460-nm absorption line could be observed by a handheld prism spectroscope. The range of the relative density varied between 3.93 and 4.07. Detailed results are shown in Table I.

Trace Elements

The test results of LA-ICP-MS are shown in Table II. After analyzing the changes of each element, the iron content was the highest among impurity elements, and it has the closest relation to zoning color, which is one of the most important coloring ions in sapphire. This means that the presence of iron could have influenced the chemical composition, physical properties, and crystal structures of sapphire. Table II shows that the iron content in the samples was between 1.40% and 2.00%. For sample SC1, iron content of zoning core, the darkest area of sample SC1, was more than 2.00%, which was significantly higher than the other positions of the sample. Figure 3 shows the distribution of iron elements of sample SC1 and SC2. Corresponding to the dotting sequence from 1 to 5, which was set to start from the zone core to alternate deep-colored and light-colored bands in sample SC1, while the dotting order was set to be alternatively deep-colored and light-colored bands in sample SC2. Overall, starting from the zoning core to the edge, iron content gradually decreased. The iron content in deep-colored band is higher than that in light-colored band. For sample SC2, the iron content changed regularly with the band color.

Titanium is also one of the important coloring elements in sapphire. Ti^{4+} replaces Al^{3+} in the sap-

Table I. Conventional testing results

Sample	Weight (g)	Color	Refractive index	Dichroism	Absorption spectrum	Relative density
SC1	0.41	Deep blue	1.762–1.770	Blue–greenish-blue	450-nm absorption band, 460 absorption line	3.99
SC2	0.40	Greenish-blue	1.763–1.771	Blue–greenish-blue	450-nm absorption band, 460 absorption line	4.07
SC3	0.71	Deep blue	1.76	Blue–greenish-blue	450-nm absorption band, 460 absorption line	3.93
SC4	0.29	Greenish-blue	1.763–1.772	Blue–green	450-nm absorption band, 460 absorption line	4.00

phire crystal lattice. With the presence of Fe^{2+}, both Fe^{2+} and Ti^{4+} work together to form the blue color of sapphire. Table II shows that most titanium content of the samples was in the range of 0.02% and 0.06%. In one sample with zoning, the titanium content value of the zoning core was higher than any other position. Overall, the titanium content directly correlated with the iron content.

Ga^{3+} has a similar ionic radius with Al^{3+}, and they have the same electrovalence. Gallium exists extensively in sapphire as an isomorphism. Gallium contents in basalt and metamorphic sapphire have distinguishable significance. In 53.3% of the samples, the gallium content was about 2.60×10^{-2} %, in which the zoning core had the highest gallium content. Mary Isabelle Garland[13] put forward that the content of elemental gallium had genetic significance; the gallium content of metamorphic rock type sapphire is less than 0.01%, and the gallium content of basalt type sapphire is higher than 0.01%, which is consistent with the data in this article.

In the zoning core of sample SC1, not only was iron content the highest, but also a variety of trace elements were the highest in all four samples. Overall, compared with sapphire from other places,[17] Shandong sapphire is rich in Fe, Cu, Mn, Cr, and V, and it is low in alkali metal elements, which is detectable in most samples.

Raman Spectrum

Fe^{3+} and Cr^{3+} are the impurity ions in corundum that exist in the crystal lattice in the form of isomorphism.[18] They have the same Raman active vibration mode. When the bond force vibration constants are different, the spectrum will produce different Raman shifts. Al_2O_3, Fe_2O_3, and Cr_2O_3 of α-Al_2O_3–type materials have different Raman shifts,[19] as shown in Table III.

Figure 4 shows the Raman spectrum of SC1, which clearly indicates that the intensity of Raman spectrum is stronger in zoning core and deep-colored bands, and it is weaker in light-colored bands. Besides the spectrum peaks caused by Al^{3+} and O^{2-} of Al_2O_3 with the comparison of the Raman spectra in Fig. 4, the spectrum peaks at 246 cm^{-1} caused by Fe^{3+} vary with the band color. The peak intensity of 246 cm^{-1} changes regularly with iron content (Table II). Figure 5 shows the Raman spectrum of SC2, in which the deep-colored band shows slightly stronger Raman spectrum intensity than the light-colored band. Obviously, the intensity of Raman spectrum of different color bands varies in the strength of Raman peak at 244 cm^{-1}, which is caused by the substitution of Fe^{3+} for Al^{3+}. Most peak positions have slight deviation because of the impurities in sapphire. Two spectrum peaks can be observed at 471 cm^{-1} and 705 cm^{-1} in Fig. 4, which cannot match with Raman spectrum of Al_2O_3, Fe_2O_3, or Cr_2O_3. There is no perfect interpretation on the two peaks, which requires further study to complete Raman research on sapphire.

DISCUSSION

The Valence State of Fe

The zoning core of Shandong sapphire is dark blue where the highest iron content is over 2.00%. The content of iron is higher in deep-colored bands than in light-colored ones. Similarly, the strength of Raman spectrum peaks caused by Fe^{3+} varies with band color, which is also directly correlated to the total iron content.

When iron concentration is in excess of 1%, it has a significant effect on the Raman spectrum.[20] In a certain range, the effect of impurity elements on Raman spectrum is mainly reflected in peak intensity. The average content of total iron is about 1.5%, and the changes of peak intensity caused by Fe^{3+} are directly related to the total iron content. Compared with Raman spectra of synthetic forsterite and natural olivine, the presence of Fe^{2+} will cause weak-medium intensity of 426 cm^{-1} Raman shift.[21] In contrast, Shandong sapphire samples presented in this article have no Raman shift at 426 cm^{-1}. This finding further proves that in Shandong sapphire, the content of Fe^{2+} is relatively low. In summary, iron is dominated by Fe^{3+} in Shandong sapphire.

Origin of Zoning

Based on the newly obtained analytical results of zonal sapphire in this study, combined with previous studies on the formation of Shandong sapphire [22,23]

Table II. The result of elements of shandong sapphire analyzed by LA-ICP-MS (10^{-4} wt.%)

Element	SC1-1	SC1-2	SC1-3	SC1-4	SC1-5	SC2-1	SC2-2	SC2-3	SC2-4	SC2-5	SC3	SC4	Detection Limit[27] (n = 10, 3 s)
Si	2130.00	11187.00	bdl	8415.00	1565.00	bdl	7042.00	233.40	bdl	635.40	4838.00	5140.00	1
Ti	901.70	271.00	167.40	221.00	107.70	562.40	549.90	960.50	434.20	509.10	329.00	288.10	0.001
Al	975,864	971,418	988,572	975,258	986,795	983,451	974,213	980,012	984,485	980,354	980,668	975,125	0.006
Fe	20,533	16,601	14,140	14,976	11,433	17,307	16,936	18,121	15,246	17,959	14,041	18,730	0.002
Mg	201.50	50.46	78.46	105.60	61.46	96.39	111.20	53.61	47.38	84.31	63.73	29.01	0.005
Ca	50.44	177.40	bdl	621.50	bdl	207.30	745.90	239.40	314.50	230.00	bdl	409.30	0.05
Mn	bdl	bdl	6.57	bdl	bdl	11.39	4.31	bdl	0.36	1.57	2.81	7.57	0.0001
Na	bdl	bdl	bdl	bdl	362.50	482.20	bdl	675.10	bdl	bdl	bdl	156.40	0.03
K	26.30	14.17	41.56	bdl	17.68	0.72	8.16	29.38	41.68	bdl	bdl	bdl	0.004
V	23.77	13.92	13.15	15.38	18.63	15.00	17.18	18.67	14.99	18.91	22.64	9.99	0.09
Cr	bdl	bdl	51.17	108.80	169.60	bdl	38.47	bdl	85.22	bdl	30.36	168.60	11
Co	1.33	0.99	1.10	3.07	bdl	0.96	0.04	0.55	1.02	2.84	0.80	0.10	0.7
Ni	72.44	29.19	24.43	bdl	bdl	113.50	71.15	86.86	bdl	bdl	bdl	bdl	0.4
Cu	13.61	5.66	bdl	22.39	5.08	1.12	bdl	4.21	bdl	bdl	8.25	bdl	0.5
Zn	28.04	bdl	25.06	49.51	0.02	0.13	14.18	2.55	bdl	bdl	bdl	bdl	1
Ga	325.30	281.30	254.50	276.70	260.30	262.20	260.00	265.20	263.50	261.50	300.40	262.00	0.1
Nb	15.13	bdl	0.63	bdl	0.18	1.7	1.72	bdl	bdl	bdl	0.11	bdl	0.01
Sn	12.23	14.83	18.66	bdl	19.03	9.14	0.58	1.74	0.96	bdl	2.12	16.31	1
Ba	7.92	bdl	4.10	13.54	bdl	bdl	bdl	bdl	2.79	bdl	3.66	1.85	0.04
Ta	51.02	bdl	1.19	0.58	0.73	0.66	0.53	bdl	0.37	bdl	bdl	0.20	0.005
Pb	0.84	bdl	1.79	1.45	0.60	0.65	1.55	0.06	bdl	bdl	bdl	0.34	0.05

bdl below the detection limit

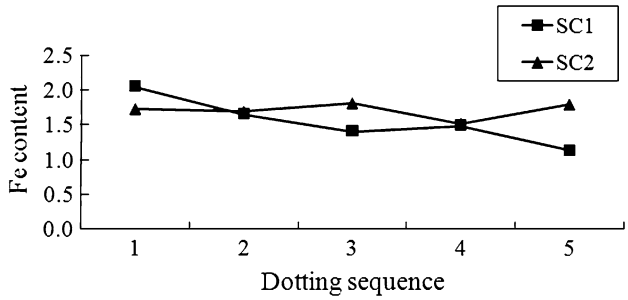

Fig. 3. Distribution of iron elements of sample SC1 and SC2.

Table III. The Raman shifts of different vibration modes for Al_2O_3, Fe_2O_3, and Cr_2O_3 powder

		Frequency (cm^{-1})		
Description		**Al_2O_3**	**Fe_2O_3**	**Cr_2O_3**
O^{2-} axial displacement	A_1g	645	500	550
	Eg	751	612	609
O^{2-} diagonal displacement	Eg	578	413	530
O^{2-} displacement $\perp L^2$	Eg	451	298	397
R^{3+} displacement	A_1g	418	226	303
	Eg	432	293	351
	Eg	378	245	

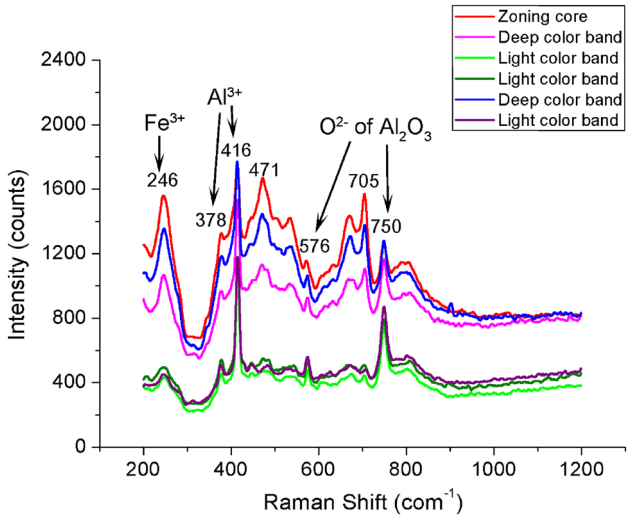

Fig. 4. Raman spectrum of SC1.

and its zoning characteristics,[24–26] the zoning core of Shandong sapphire is rich in impurity elements. As Shandong sapphire commonly develops zones beginning from the zoning core to the edge, the content of iron and titanium decreases gradually overall while displaying periodic variation with changes in band color. The zoning core is usually dark blue or nearly black, in which there are deposits the highest amount of the impurities of Fe, Ti, Ni, Cu, Ga, Ta, Ba, and so on. The changes in impurity concentrations in

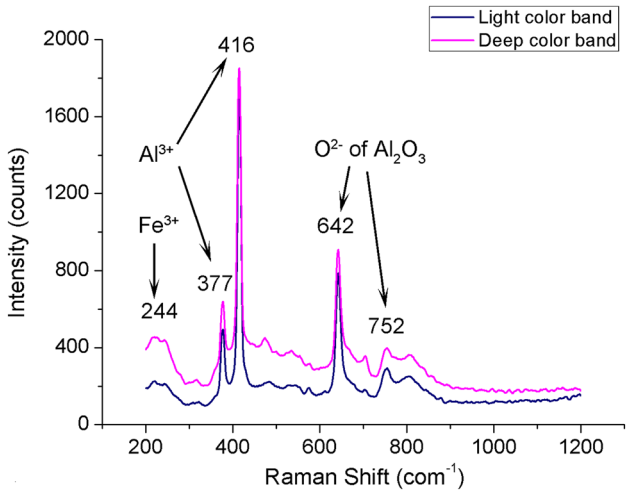

Fig. 5. Raman spectrum of SC2.

zonal sapphire indicate that the parent magma composition of sapphire formation environment changes in volatility. In the environment of high temperature (and/or pressure), the core part of sapphire crystal forms and a large amount of iron is free, whereas the magma is rich in trace elements, forming the core part of sapphire zoning with high concentrations of impurity elements. After a period of time, the temperature (and/or pressure) of crystallization environment begins to decrease, reaching the crystallization condition of some minerals, and the corresponding elements of Fe, Ti, and other trace elements enter the minerals. If the magma concentration of these elements is significantly lower, then fewer impurity elements enter the sapphire crystal lattice, forming light-colored bands. After a while, the temperature (and/or pressure) of the parent magma increases again, without reaching the melting point of sapphire, but it is higher than that of the minerals containing iron and part of the elements of Ni, Cu, Ga, Ta, and Ba, and so on. Some of the crystallized minerals dissolve in magma. Thus, the magma is rich in these elements once again, and the deep-colored band forms. This process repeats, and Shandong sapphire forms dark blue core with deep- and light-colored bands.

CONCLUSION

In this study, the zoning features of Shandong sapphire is characterized by LA-ICP-MS and Raman spectrometry. The iron content in the zoning core is more than 2.00% in the darkest area of the sapphire. Also, the iron content is significant higher in deep-colored bands than in light-colored bands, which shows that the total iron content has an important impact on the color of sapphire.

The intensity of Raman spectrum peaks caused by Fe^{3+} varies with the band color, and it is directly correlated with the total iron content. The results from LA-ICP-MS and Raman spectrum led to the

conclusion that iron is dominated by Fe^{3+} in Shandong sapphire.

In the growth of Shandong sapphire, changes in temperature (and/or pressure) lead to changes in the parent magma composition and cause zoning formation, whereas the band color is directly related to periodic changes in the Fe^{3+} content. Sapphire zoning is an intuitive reflection on the changes of parent magma, indicating that the composition and condition in the upper mantle are not stable. With highly sensitive testing technologies, chemical study on the zonal sapphire reveals that the parent basalt magma has periodic variations in its component content. Further study on zonal sapphire is still needed to examine the sapphire origin.

ACKNOWLEDGEMENTS

The authors acknowledge contributions in terms of helpful discussion and Raman experiment, with grateful thanks to Fei Liu of Chinese Academy of Geology Science and Hongyun Yu of Research Center of Material Science, Tsinghua University.

REFERENCES

1. J.X. Sun, F. Li, Y.S. Dang, G. Cui, and X.B. Zhou, *Acta Petrol. Mineral.* 24, 62 (2005).
2. L.S. Wang, *Mineralogical Study the Causes of Chinese Gem Corundum Deposit Types, Distribution Cum Fuping Group Metamorphic Corundum Gemstone Deposits* (Beijing: China University of Geosciences, 1996), p. 20.
3. W.K. Guo, L.S. Liu, and Z.J. Yu, *Mineral Depos.* 5, 1 (1982).
4. X.Y. Yu, X.M. Yao, and P. Han, *Geol. Prospect.* 36, 28 (2000).
5. Z.X. Dong, L.F. Yang, and Y.W. Wang, *Bull. Chin. Acad. Geol. Sci.* 20, 177 (1999).
6. G.W. Bowersox, E.E. Foord, and B.M. Laurs, *Gems Gemol. Summer* 36, 110 (2000).
7. A.R. Moon and M.R. Phillips, *Sci. Alumin.* 77, 356 (1994).
8. V. Pisutha-Arnond, T. Häger, W. Atichat, and P. Wathanakul, *J. Gem.* 30, 131 (2006).
9. F.L. Sutherland and D. Schwarz, *Austral. Gemmol.* 21, 30 (2001).
10. V. Garnier, D. Ohnenstetter, G. Giuliani, A.E. Fallick, T.P. Trong, V.H. Quang, L.P. Van, and D. Schwarz, *Mineral. Mag.* 69, 21 (2005).
11. Z.L. Dong, X.M. Chen, W.X. Hu, R.C. Wang, and M. Zhao, *Acta Petrol. Sinica* 23, 805 (2007).
12. Y.C. Song, W.X. Hu, and W.L. Zhang, *Acta Petrol. Mineral.* 27, 489 (2008).
13. M.I. Garland (Ph.D. dissertation, University of Toronto, Ontario, Canada, 2002), p. 137.
14. A. Abduriyim and H. Kitawaki, *J. Gemm.* 30, 23 (2006).
15. A.H. Rankin, J. Greenwood, and D. Hargreaves, *J. Gemm.* 28, 473 (2003).
16. H.P. Longerich, S.E. Jackson, and D. Günther, *J. Anal. Atom. Spectrom.* 9, 899 (1996).
17. S. Saminipanya, D.A.C. Manning, and G.T.R. Droop, *J. Gemm.* 28, 399 (2003).
18. E.B. Wilson, Jr., J.C. Decius, AND P.C. Cross, *The theory of the Molecular Vibration, Infrared and Raman spectrum*, 1st ed. (New York: Dover publications, 1980), p. 185.
19. V.C. Farmer, *Infrared Spectrum of Minerals* (London: Mineralogical Society, 1982), p. 235.
20. G.Z. Wu, *Molecular Vibrational Spectroscopy: Theory and Principle* (Beijing: Tsinghua University Press, 2001), p. 89.
21. J.L. Fan, S.G. Guo, J. Mao, and L.Y. Shi, *Appl. Laser* 27, 209 (2007).
22. Z.H. Ding, *Acta Mineral. Sinica* 29, 442 (2009).
23. Y.C. Song and W.X. Hu, *Acta Petrol. Mineral.* 28, 349 (2009).
24. P.X. Wu, J.P. Wu, W.D. Xiao, and C.W. Li, *Geol. Geochem.* 4, 40 (1997).
25. F.Y. Wu and Q. Lin, *Acta Petrol. Mineral.* 12, 126 (1993).
26. J.Z. Niu, Y. Liu, and Y.J. Di, *Acta Petrol. Mineral.* 33, 102 (2014).
27. M.Y. Hu, H.H. Liao, X.C. Zhan, X.T. Fan, G. Wang, and Z.R. Jia, *Chin. J. Anal. Chem.* 7, 950 (2008).